

# Single-Epoch Ambiguity Resolution for Highway and Racetrack Applications

James W. Sinko, *SRI International*

## BIOGRAPHY

James W. Sinko is a Principal Engineer at SRI International. He received his B.S. (Engineering Science) and MSEE from Stanford University, and his Ph.D. (EE) from the University of Rochester. Dr. Sinko has been with SRI since 1967, working with radar and aircraft systems. For the last 8 years, he has been working with precision GPS for military and civil applications.

## ABSTRACT

The development of reliable real-time kinematic (RTK) GPS on most highways will enable many safety and convenience applications, such as lane departure warning. Eventually, GPS could play an important role in fully automated highways. On the racetrack, RTK GPS can show car handling characteristics and driver performance to high precision.

Real-time centimeter-level accuracy GPS for highway and motor racing applications requires specialized algorithms and L1/L2 receivers. The greatest difficulty encountered with this system is the frequent obscurations that cause the receiver to lose track of the signal. This results in a loss of the L2 carrier phase for many seconds (test results for a few popular brands of receivers are included), and even after track is reestablished, the accuracy is degraded for a couple of seconds.

The term single-epoch ambiguity resolution is somewhat of a misnomer in that GPS receivers do have smoothing filters that introduce a significant correlation between successive epochs when sampling rates are 1 Hz or higher, and multipath errors are highly correlated in time. In this paper, autocorrelation functions for the residuals after correct ambiguity resolution are shown. The single-epoch method eliminates the prolonged carrying of incorrect integer solutions that occasionally occurs with Kalman filter and other multiple-epoch algorithms. After

encountering an obstacle, the single-epoch method provides a solution as soon as the receiver recovers an adequate number of signals, although the probability of selecting the correct integers will improve after the receiver has had a few seconds of settling time. Over short baselines (a few kilometers) and with six or more satellites available, ambiguities are resolved correctly over 99% of the time. In clear areas, such as the Buttonwillow, California, racetrack, correct single-epoch ambiguity resolution has been demonstrated over 99.8% of the time.

Vehicular applications can use altitude aiding to help significantly in resolving the ambiguities. Code differential GPS gives the location on the road with sufficient accuracy so that an accurate height can be found from a detailed road database and used as a constraint in finding the solution. The algorithm has been tested in a series of rooftop static tests during which the antennas were covered for short periods of time. On a relatively clear stretch of freeway with only one overpass, correct ambiguity resolution was demonstrated 88% of the time without altitude aiding and 96% of the time with altitude aiding. Over a more obscured stretch of freeway with trees and hills, ambiguities were correctly resolved 62% of the time without altitude aiding and 91% of the time with altitude aiding.

## INTRODUCTION

Low to moderate accuracy GPS automotive applications such as navigation, vehicle tracking, stolen vehicle tracking, time-dependent toll collection, adaptive lighting, suspension, drive train control, curve warning, rear collision warning, and intersection collision warning can be implemented with current code-based GPS technology. Other applications requiring knowledge of which lane a car is in can marginally be done with code differential GPS. These applications include situation awareness displays (that

show all surrounding vehicles and their relative velocities, especially those in blind spots), and adaptive cruise control (ACC) determination of which lane the lead vehicle is in. Navigation is also enhanced by knowledge of which lane the vehicle is in because the driver can be advised to shift lanes for an upcoming turn. However, the highest payoff GPS automotive applications require centimeter-level accuracy. These applications include lane departure warning and lanekeeping (GPS/inertial measurement unit [IMU]-based steering), ultimately leading to fully automated highways. RTK GPS is clearly accurate enough for all these applications, and the applications will be more robust with the use of RTK GPS. (A more extensive discussion of near to medium term highway applications appears in Venhovens et al. [1998].) L1/L2 GPS receivers are virtually necessary for RTK by permitting use of widelane phase to enable single-epoch ambiguity.

Auto racing is beginning to use GPS for analyzing how a car and driver are performing and for enhancing the televised coverage of races (continually monitoring and displaying speeds and time gaps between cars). As well as analyzing car and driver performance, RTK GPS can give a historical tracking of all cars on the track for scoring purposes and to resolve rule infractions such as excessive speeds in pit row and cutting below apron lines. Many apron infractions are the result of being forced low by another car; RTK GPS can aid in resolving these disputes.

The rulings of various sanctioning bodies will affect the future of RTK GPS in motor racing. Most of these bodies impose technology limits on the race cars to prevent a few wealthy teams from dominating. RTK GPS could become a victim of these policies. On the other hand, if L1/L2 receiver prices fall enough, the use of RTK GPS for scoring may become less costly than the transponder-based systems currently used for scoring races.

Most RTK software and most dual frequency civilian receivers have been designed to operate in a relatively clear environment for surveying applications or for agricultural vehicles. Freeways and many racetracks require that RTK GPS work when large numbers of obstructions (overpasses, signs, other vehicles, hills, trees, and buildings) are present. A number of steps can be taken to improve the ability of RTK software to recover quickly from these obstructions (some receivers perform better than others in such recovery). Single-epoch ambiguity resolution algorithms are especially useful for rapidly recovering from obstructions. Map-derived altitude aiding (deriving height information from a code-derived position

and an accurate map of the road that gives height) has also been proven very useful. "Satellite snooping," testing the solution with a satellite removed, is useful for removing satellite signals that are corrupted from severe multipath or phase distortion.

Current problems for such vehicular augmentations include obstacles, integrity, and cost. C/A code on L2 will help the recovery time after encountering obstacles. L5 will increase the availability and reliability of integer ambiguity resolution, and, when combined with inertial systems, may provide a reasonable measure of integrity. The realization of the Galileo system would provide more satellites, which is helpful for overcoming obscurations. Many obstacle situations will require that inertial and/or wheel sensor measurements be incorporated into the system. Additional sensors such as vision systems and magnetic nails could be used in conjunction with RTK GPS. These additional sensors can also aid in establishing integrity.

## FORMULATION

The single-epoch formulation is similar to that in Taniura et al. [1998] (see Eq. 1 that follows). The left side of the equation consists of the measured values minus the calculated values. The measured values include the double difference L1 phases, widelane phases, and pseudoranges. The unknown vector on the right-hand side of the equation will have the incremental changes (between each iteration) of the positions of the rover,  $x$ ,  $y$ ,  $z$ , L1 integers ( $N_1, \dots, N_4$ ), and widelane integers ( $N_{w1}, \dots, N_{w4}$ ).

L15 is the measured L1 double difference phase between satellite vehicles (SVs) 1 and 5, where 5 is the pivot SV,  $\rho_{15}$  is the computed double difference range,  $W_{15}$  is the measured double difference widelane phase, and  $P_{15}$  is the measured double-difference pseudorange. The last element of the left-hand vector and the last row of the design matrix are used only in the case of altitude aiding (see below).  $H_m$  is the height found from the map, and  $H$  is the computed height. The difference between the rover and reference station is implied in all measured and calculated variables, but not explicitly shown. For simplicity, a minimum number of satellites (5 in this case) is shown. For a more typical 7 available SVs, thus 6 double differences, the left-hand vector will be  $19 \times 1$ , the design matrix will be  $19 \times 15$ , and the unknowns vector will be  $15 \times 1$ . If altitude aiding is not used, the corresponding dimensions would be  $18 \times 1$ ,  $18 \times 15$ , and  $15 \times 1$ .

$$\begin{bmatrix} L_{15} - \rho_{15} \\ L_{25} - \rho_{25} \\ L_{35} - \rho_{35} \\ L_{45} - \rho_{45} \\ W_{15} - \rho_{15} \\ W_{25} - \rho_{25} \\ W_{35} - \rho_{35} \\ W_{45} - \rho_{45} \\ P_{15} - \rho_{15} \\ P_{25} - \rho_{25} \\ P_{35} - \rho_{35} \\ P_{45} - \rho_{45} \\ H_m - H \end{bmatrix} = \begin{bmatrix} \partial\rho_{15}/\rho_x & \partial\rho_{15}/\rho_y & \partial\rho_{15}/\rho_z & \lambda_1 & 0 & 0 & 0 & 0 & 0 & 0 & 0 & 0 \\ \partial\rho_{25}/\rho_x & \partial\rho_{25}/\rho_y & \partial\rho_{25}/\rho_z & 0 & \lambda_1 & 0 & 0 & 0 & 0 & 0 & 0 & 0 \\ \partial\rho_{35}/\rho_x & \partial\rho_{35}/\rho_y & \partial\rho_{35}/\rho_z & 0 & 0 & \lambda_1 & 0 & 0 & 0 & 0 & 0 & 0 \\ \partial\rho_{45}/\rho_x & \partial\rho_{45}/\rho_y & \partial\rho_{45}/\rho_z & 0 & 0 & 0 & \lambda_1 & 0 & 0 & 0 & 0 & 0 \\ \partial\rho_{15}/\rho_x & \partial\rho_{15}/\rho_y & \partial\rho_{15}/\rho_z & 0 & 0 & 0 & 0 & \lambda_w & 0 & 0 & 0 & 0 \\ \partial\rho_{25}/\rho_x & \partial\rho_{25}/\rho_y & \partial\rho_{25}/\rho_z & 0 & 0 & 0 & 0 & 0 & \lambda_w & 0 & 0 & 0 \\ \partial\rho_{35}/\rho_x & \partial\rho_{35}/\rho_y & \partial\rho_{35}/\rho_z & 0 & 0 & 0 & 0 & 0 & 0 & \lambda_w & 0 & 0 \\ \partial\rho_{45}/\rho_x & \partial\rho_{45}/\rho_y & \partial\rho_{45}/\rho_z & 0 & 0 & 0 & 0 & 0 & 0 & 0 & \lambda_w & 0 \\ \partial\rho_{15}/\rho_x & \partial\rho_{15}/\rho_y & \partial\rho_{15}/\rho_z & 0 & 0 & 0 & 0 & 0 & 0 & 0 & 0 & 0 \\ \partial\rho_{25}/\rho_x & \partial\rho_{25}/\rho_y & \partial\rho_{25}/\rho_z & 0 & 0 & 0 & 0 & 0 & 0 & 0 & 0 & 0 \\ \partial\rho_{35}/\rho_x & \partial\rho_{35}/\rho_y & \partial\rho_{35}/\rho_z & 0 & 0 & 0 & 0 & 0 & 0 & 0 & 0 & 0 \\ \partial\rho_{45}/\rho_x & \partial\rho_{45}/\rho_y & \partial\rho_{45}/\rho_z & 0 & 0 & 0 & 0 & 0 & 0 & 0 & 0 & 0 \\ \partial H/\rho_x & \partial H/\rho_y & \partial H/\rho_z & 0 & 0 & 0 & 0 & 0 & 0 & 0 & 0 & 0 \end{bmatrix} \times \begin{bmatrix} x \\ y \\ z \\ N_1 \\ N_2 \\ N_3 \\ N_4 \\ N_{w1} \\ N_{w2} \\ N_{w3} \\ N_{w4} \end{bmatrix} \quad (1)$$

The weighting matrix P allows the use of different standard deviations for each SV. It is formed from three separate submatrices, one for L1, one for widelane, and one for pseudorange:

$$P = \begin{bmatrix} \Sigma_{L1}^{-1} & 0 & 0 & 0 \\ 0 & \Sigma_{WL}^{-1} & 0 & 0 \\ 0 & 0 & \Sigma_{PR}^{-1} & 0 \\ 0 & 0 & 0 & \sigma_h^{-2} \end{bmatrix}, \quad (2)$$

where  $\sigma_h$  is the height standard deviation (when altitude aiding is used). The three submatrices are of the form

$$\Sigma = \begin{bmatrix} 2\sigma_1^2 + 2\sigma_5^2 & 2\sigma_5^2 & 2\sigma_5^2 & 2\sigma_5^2 \\ 2\sigma_5^2 & 2\sigma_2^2 + 2\sigma_5^2 & 2\sigma_5^2 & 2\sigma_5^2 \\ 2\sigma_5^2 & 2\sigma_5^2 & 2\sigma_3^2 + 2\sigma_5^2 & 2\sigma_5^2 \\ 2\sigma_5^2 & 2\sigma_5^2 & 2\sigma_5^2 & 2\sigma_4^2 + 2\sigma_5^2 \end{bmatrix}, \quad (3)$$

where 5 is the pivot satellite, and  $\sigma_i$  is the standard deviation of the L1 phase, widelane phase, or pseudorange (depending on submatrix) of the *i*th satellite. The submatrices are derived using the methods outlined in Leick [1995]. For the five-SV case, the P matrix is 13×13 when altitude aiding is used. The resulting minimization problem to obtain the float solution is solved as in Taniura et al. [1998]. The float solution and covariance matrix are then processed using the Lambda method of integer ambiguity resolution (see Teunissen [1994], and De Jonge and Tiberius [1996]).

By using a differential code-based solution, and an accurate road map or database that contains accurate road heights, and knowing the height of the antenna on the vehicle, height above the ellipsoid can be determined to within a few centimeters before attempting to find the RTK solution. To use altitude in aiding the solution, an extra measured minus calculated (height) is added in the list of measured minus calculated on the left-hand side of Eq. 1. In the design matrix, a row is added that has non-zero values for only the first three columns, namely, the partial derivatives of height with respect to x,y,z. This

formulation has been shown to increase appreciably the availability of the RTK solution.

Although the resulting matrix operations appear to be larger than in most RTK software, the program runs approximately 100 times faster than real time when 1 Hz data are being processed on a 200 MHz Windows-based laptop.

Satellite snooping is a technique suggested by Taniura et al. [1998]. This method is based on evidence that difficulties resolving ambiguities frequently can be traced to a single satellite. This satellite is not easy to identify, so the test repeats the solution as many times as there are satellites, each time with a single satellite removed. If a solution with a satellite removed has a substantially lower ratio of the square sum of the residuals of the best set of integers to the second best set, it is selected.

## VERIFICATION

Generally, truth has been obtained by monitoring a combination of height and the integer ambiguities. In many cases, the height difference between the reference and rover antennas is measured with a tape measure at the beginning and end of a run when the rover is close to the reference station. When altitude aiding is not being used, an error in resolving the ambiguities usually shows up as an unreasonable jump in height, given that most roads are quite smooth. In tests with simulated outages, a second receiver that is not switched off is able to give data to corroborate the solution derived from the test receiver. When altitude aiding is being used, the task of verifying the computations becomes more difficult, since the height computation is forced to be near the correct answer. Path deviations of 20 cm are common for careful road driving. Race car drivers frequently have even larger deviations when exiting corners, and smaller deviations on other parts of the track. Thus, path deviations of manually driven cars are of use in determining the performance RTK GPS solutions because wrong integers usually cause errors larger than 20 cm. However, more accurate

measurements are desirable. In California, path deviations combined with examination of integers was used to determine the results for the Morgan Hill and I280 altitude aiding experiments. The I280 experiments also relied on the noise produced by tires hitting the Bott's dots (the raised markers between lanes) to demonstrate the accuracy of the RTK GPS solutions.

Other approaches (not used here) to testing would be to use a rail vehicle so the lateral deviations are smaller, or a video camera system looking for deviations from a line. The use of magnetic nails (markers) in the road with magnetometers in the vehicle has been used by Yang et al. [2001].

Table 1 provides a summary of a number of tests that have been done with a multi-epoch least squares algorithm (LSME) and those done with the single-epoch algorithm (SE). The abbreviation AA is for map-based altitude aiding and SS is for satellite snooping. The missed data can be because of an insufficient number of satellites. Epochs where one of the receivers did not send a message because of communications overloads were ignored—these missed records are isolated events causing only a single epoch to be missed and occur less than one percent of the time. Distance to the reference station for all these experiments was less than 4 km.

### Morgan Hill US101 and I280 Tests

These earlier experiments were conducted with a previous software version that used a multi-epoch least squares ambiguity resolution software based on the method of Hatch [1990]. The Morgan Hill freeway consisted of a 3 km loop where the exits were arranged such that the vehicle never passed beneath an overpass. The only significant obstacles were exit signs and light poles. A 6 km stretch of I280 located near Stanford University was chosen as a more typical freeway environment. This roadway is located in rolling hills and at least some of the satellites were frequently masked by trees or embankments. Most of the I280 experiments were done using a real-time system. The northern exit passed over the freeway so the sky was not blocked there, and while the southern exit did cause a sky blockage, this portion of the loop was not included in the tabulations because the radio link for the real-time corrections would not work in that area.

As shown in Table 1, the primary lesson of these experiments is that map-derived altitude aiding can appreciably enhance the availability of correct ambiguity resolutions. The altitude maps for these experiments were made by manually selecting the best of multiple probe vehicle runs during times when favorable satellite geometries were available. Both of these experiments are described in more detail in Sinko et al. [1999].

**Table 1:** Summary of Testing Results

Location	Description	Algorithm	% Missed	% Wrong	% Right
Morgan Hill	Clear freeway—signs	LSME			88
Morgan Hill	Clear freeway—signs	LSME+AA			96
I280	Freeway, hills, trees, signs	LSME			62
I280	Freeway, hills, trees, signs	LSME+AA			91
Buttonwillow	Clear racetrack	SE	0	0.2	99.8
Gilroy	Mostly clear freeway, some trees, one overpass	SE	5.9	0.2	93.9
San Carlos	Clear parking area, poor satellite constellation (5–7 SVs)	SE	0	2.5	97.5
San Carlos	Clear parking area, poor satellite constellation (5–7 SVs)	SE+SS	0	1.1	98.9
San Carlos	Clear parking area, poor satellite constellation (5–7 SVs)	SE+AA	0	0	100
San Carlos	Clear parking area, good satellite constellation (10+ SVs)	SE	0	0	100
San Carlos US101	Freeway, 4 overpasses, good satellite constellation (10+ SVs)	SE	8.0	0	92.0

### Gilroy US101 Test

This experiment was designed to test the response of RTK GPS to an overpass. It consisted of a single overpass in the middle of a freeway loop. At the north and south ends, course reversals could be made by crossing over the freeway on overpasses. The obscuring overpass was encountered on both the southbound and northbound legs. In addition, the south exit had a row of trees nearby that caused RTK GPS outages. Missed epochs were because of either four or fewer SVs with proper status bits after passing under an overpass or trees at the south exit.

Figure 1 shows height as a function of latitude for four passes under the southbound overpass. The vehicle is traveling from right to left (north to south). On lap 4, there is one point that is clearly in error, based on only 5 SVs. Note that there is considerable difference in recovery time between the different passes, from 4 seconds on lap 2 to 11 seconds on lap 4.

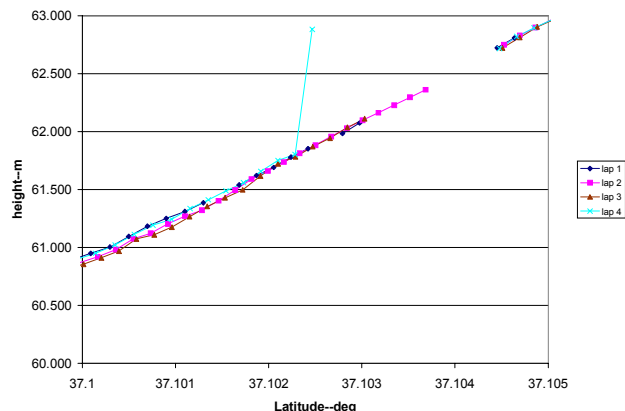


**Figure 1:** Recovery of RTK GPS after Passing Under an Overpass. Tick marks are one second apart.

### San Carlos Test

The San Carlos tests were started in a parking area with a clear view of the sky to test the receivers by introducing simulated overpasses. The experimental setup is shown in Figure 2. An overpass was simulated by opening the switch from the antenna to the test receiver. The measurements from the recovering receiver were compared with those from the receiver that was continually connected to the antenna. Data were taken at a 5 Hz rate.

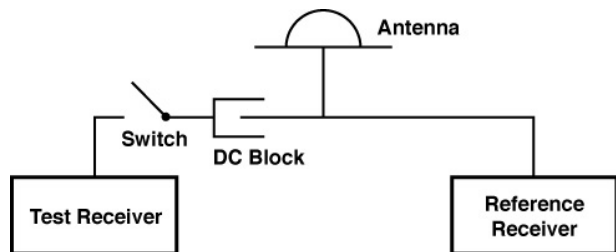


**Figure 2:** Test Setup for Simulating Obstructions

An interesting observation from the San Carlos tests is that two identical receivers using the same antenna gave appreciably different results. The receiver suffering the simulated overpasses had wrong ambiguities 0.5% of the time as compared with the other roving receiver's 2.5% wrong ambiguities (without satellite snooping). Adding satellite snooping appreciably reduced the number of wrong ambiguity resolutions, and altitude aiding (without satellite snooping) eliminated all errors. The results shown in Table 1 are all for the receiver not suffering simulated overpasses.

The vehicle path of the San Carlos US101 freeway experiment is shown in Figure 3. The epochs where solutions were obtained are denoted by markers. The blank areas are where the receiver had phase lock on four or fewer SVs after encountering an overpass. The path begins and ends in the middle of the right side. At the north end, the vehicle passes beneath an overpass, and proceeds up a cloverleaf with many trees, which causes a brief second outage. After crossing over the freeway, the vehicle again passes beneath an overpass. Another overpass is encountered southbound. The south portion of the path exits the freeway, passes over the freeway and encounters another overpass when entering the freeway. The missing data points are all because of recovery time from overpasses or trees encountered after the first overpass. Data were taken at a 1 Hz rate.

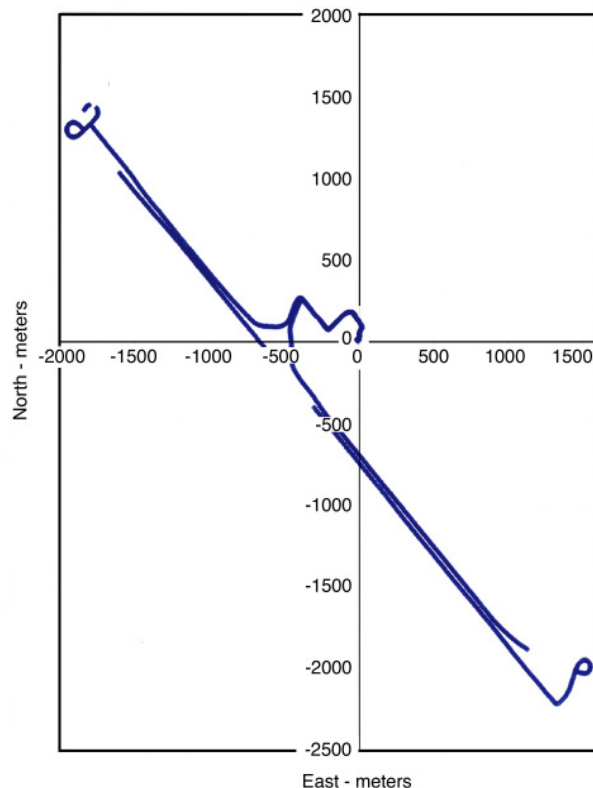


**Figure 3:** San Carlos US101 Test Path

## Buttonwillow Racetrack Tests

*Road & Track* magazine expressed an interest in using RTK GPS to aid in performing tests on cars. SRI brought dual frequency receivers, magnetic antenna mounts, and laptops for data collection to the Buttonwillow racetrack near Bakersfield, California. The track is located in a flatland area and has no obstructions, making it an ideal location for performing GPS measurements. *Road & Track* brought four new midrange sports cars (Audi TT, BMW M, Honda S2000, and Porsche Boxter S) for testing, along with Steve Millen, a former two time IMSA (International Motor Sports Association) GTS champion driver to test the cars consistently at maximum performance. Figure 4 is an RTK GPS map of the track made by driving along the edges of the Buttonwillow racetrack with a car having an antenna placed over its outside edge. Also shown on the map is the path of the Honda S2000 for four laps.

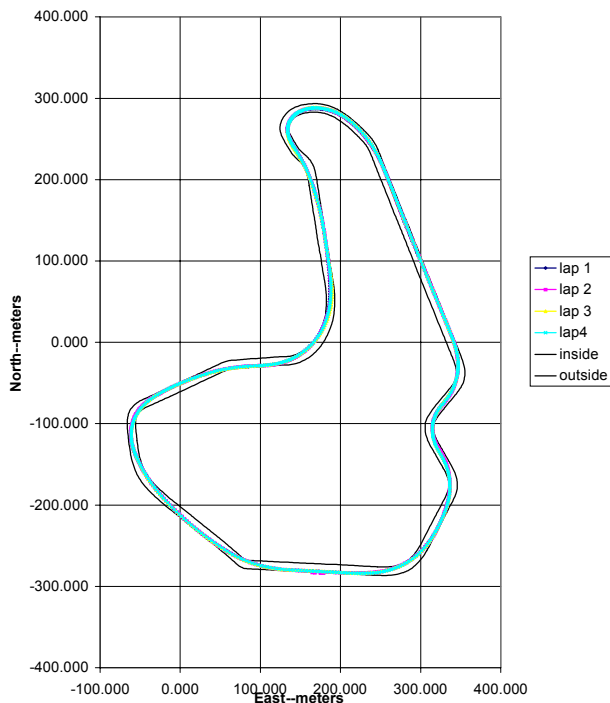


**Figure 4:** Buttonwillow East Track Map and Path of the Honda for Four Laps

The uses of GPS in motor racing are beginning to emerge. Figure 5 shows the path of each of the cars through the hairpin curve at Buttonwillow. One can clearly see the understeering characteristic of the Audi TT as compared with the other cars.

Figure 6 shows the velocity of the Honda for four laps. Note that the shift points are visible, and that the driver tried different shift points on different laps (even though all lap times were within 0.03 second of each other). On lap 2, two erroneous points cause the velocity deviations shortly before 1200 meters along the path.

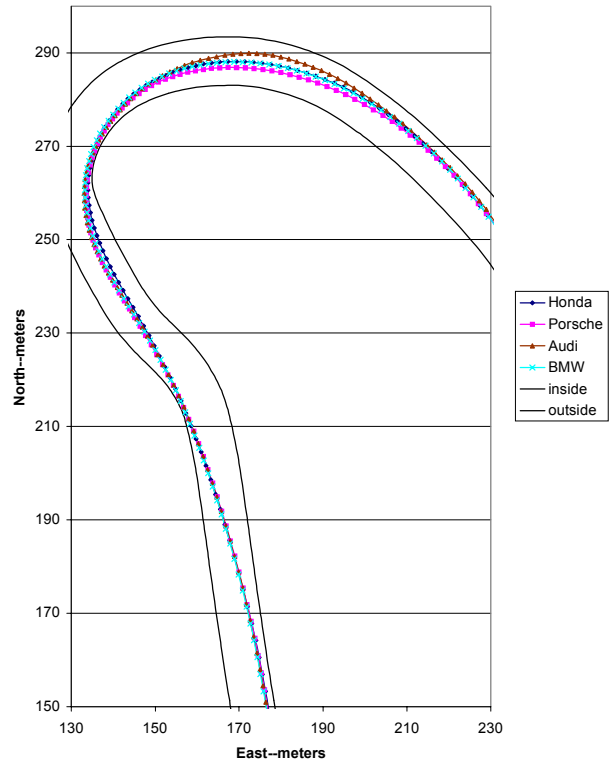


**Figure 5:** Paths of the Four Cars through the Hairpin Turn. As the cars exit the turn (upper part of the figure), the BMW and Honda paths are almost identical.

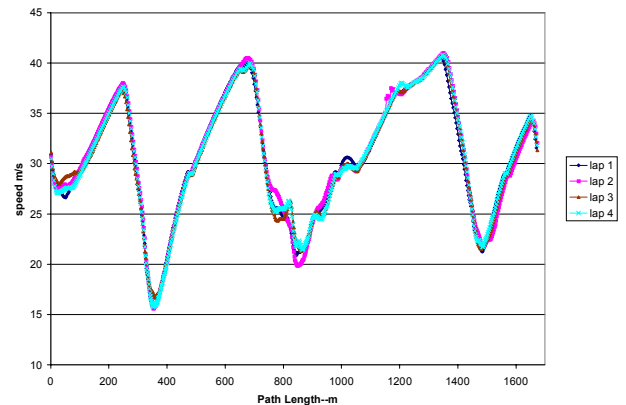


**Figure 6:** Speed Profile of the Honda for Four Laps

Figure 7 shows the lateral acceleration experienced by the GPS antenna around the hairpin curve. To derive acceleration, the velocities were differenced, an inherently noisy process. At first glance, the data appear noisy, but the high consistency of the features from lap to lap indicates that variations in road friction and rolling motion of the car are being recorded. Since the antenna is mounted about a meter above the ground, acceleration is not being measured right at the road surface. Although not quite as consistent as laps from the same car, laps from two different cars following a similar path also exhibit con-

siderable consistency of lateral acceleration curve features. Data were taken at a 10 Hz rate.

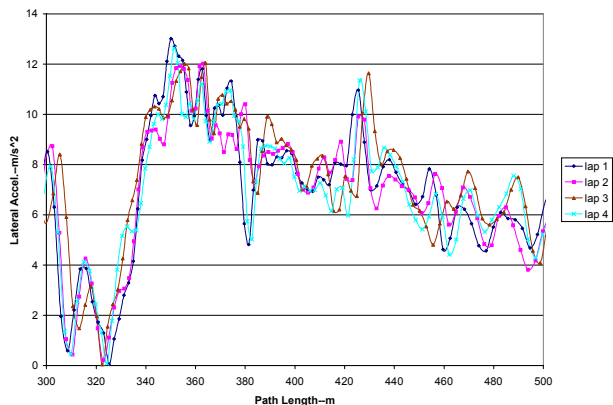


**Figure 7:** Lateral Acceleration for the Honda through the Hairpin Curve for Four Laps

Overall, 99.8 percent of measurement points had correctly resolved ambiguities. Available SVs varied from 5 to 8. In order to use altitude as a check on correct ambiguity resolution, altitude aiding was not used at Buttonwillow—all solutions were three-dimensional. In the vast majority of cases, an error in ambiguity resolution shows up as an obvious jump in altitude when examining 10 Hz data on a smooth road. The excellent view of the sky allowed a high level of correct solutions without altitude aiding. Accuracy was also verified by measuring the relative heights of the reference and rover antennas at the beginning and end of the test runs when the car was close to the reference station.

Figure 8 shows autocorrelation functions for the residual of L1 phase, the widelane phase, and the L1 code for one satellite. The strong peak at 57 seconds corresponds to the lap time. Further examination of the residuals showed that the phase residuals are very repeatable on successive laps, and that there is a high correlation between the residuals for a satellite and the heading of the vehicle. This is most likely because of phase center wander of antenna and possibly multipath. No precautions were taken to reduce

multipath—the antenna had no ground plane and was on a 6-inch post on a magnetic mount on the trunk of the cars.

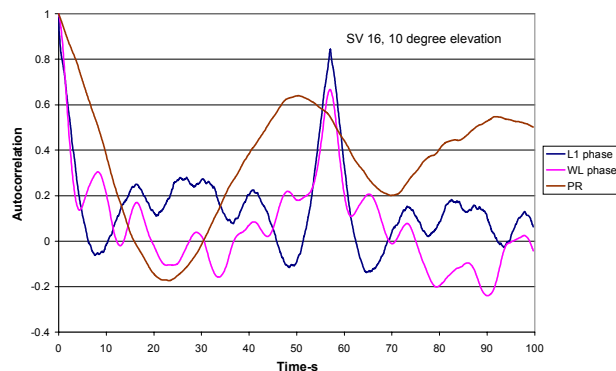


**Figure 8:** Autocorrelation Functions for the Residuals

### Receiver Tests

To ensure that the NovAtel Millenium receivers being used gave reasonable recovery times, two other receivers (a Trimble MS750 and a Navcom NCT-2000D) were tested using the arrangement in Figure 2. Table 2 shows median recovery times for the NovAtel under a variety of test conditions, and for the Trimble in a static case. Median times were chosen because the receivers had different numbers of channels, and the tests were run at different times so that the satellite constellation varied. With 10 SVs, RTK solutions were usually available by the median recovery time, but with fewer satellites an extra second or two was usually required. The Navcom had recovery times on the order of a minute (as advertised by the manufacturer) and was not further examined. The recovery time for actual overpasses and simulated overpasses appears to be comparable.

Figure 9 shows a typical recovery pattern for the NovAtel for a slightly longer obscuration time of 5 seconds. For this length of obscuration, the Trimble gave very similar results. For these longer intervals, the recovery of L2 was considerably longer than for L1. For the one- and two-second obscurations, the Trimble also behaved in this manner, but the NovAtel recovery time was usually no more than a second longer than for L1, so the recovery time for both frequencies was less than for the Trimble.

**Table 2:** Summary of Receiver Recovery Times

Receiver	Conditions	Outage Time (s)	SVs	Median Recovery Time (s)
NovAtel	San Carlos, moving, switched, clear (average of 6 tests)	0.2 to 2	10	6
NovAtel	Moving, switched, clear (average of 6 tests)	0.2 to 2	5 to 7	5
NovAtel	Moving San Carlos freeway	~1	10	10
NovAtel	Moving, Gilroy freeway	~0.5	6 to 7	6
NovAtel	Static, clear	2	7	7
Trimble	Static, clear	2	6 to 8	14

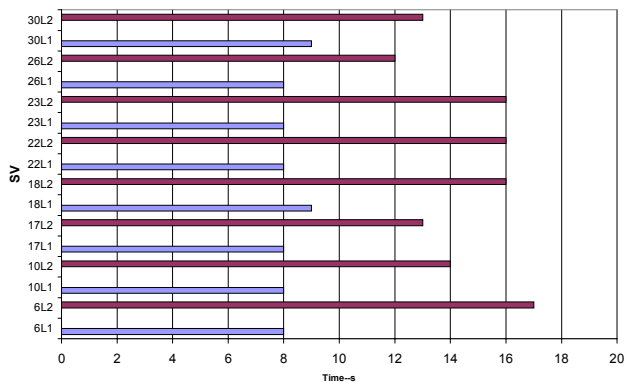


**Figure 9:** Distribution of Recovery Times for the NovAtel Receiver for a Simulated Outage

Although not used here, the L1 phase can be used to propagate location backward after full ambiguity resolution has been attained. This is useful for post-processing applications such as mapping the roads, and it is also useful for more current calibration of an IMU in a combined IMU/GPS system.

## THE FUTURE

### Applications

Further developments in the GPS constellation and user equipment will make centimeter-level location on roads and racetracks more robust. The use of C/A or other civil code on the L2 frequency will shorten the recovery time of the L2 phase. The addition of a third civil frequency will enhance the reliability of integer ambiguity resolution. As demonstrated in the two different time periods for the San Carlos data, adding more satellites can greatly enhance the reliability of centimeter-level location, especially in the presence of obstacles. If the Galileo system is deployed, the number of available satellites will almost double. The use of pseudolites can enhance the reliability of ambiguity resolution and enable the use of RTK GPS in obscured locations.

RTK GPS will need to be aided by wheel sensors and IMUs in areas where the satellites are obscured. A number of experimenters have combined RTK GPS with an IMU for highway use (see, for example, Ibrahim et al. [1999], and Yang et al. [2001]).

Systems such as magnetic nails and vision systems (both demonstrated at the Automated Highway Demonstration 1997 in San Diego) can be viewed either as alternatives to GPS or as adjuncts to GPS. Currently, it does not appear as if any of these systems can offer the versatility and reliability to be the sole system in safety-critical applications (such as vehicle steering or automated highways), rather, a combination of some of these systems will be required to attain the required availability and integrity.

Another application of RTK GPS is for situation display, a kind of air traffic control for automobiles. A heads-up display similar to that shown in Figure 10 could portray the location of all nearby vehicles. Such a display requires that most (preferably all) cars be equipped with GPS and local area communications. In the display the blue vehicle is the one having the display, the green vehicles are receding from the display vehicle (blue), and red cars are closing. The length of the arrow corresponds to the range rate at which the vehicles are approaching or receding—a long red arrow means a vehicle is rapidly getting closer. The driver can detect the red vehicle rapidly approaching from behind in the left lane without having to turn his head. He can also detect traffic events such as vehicles rapidly slowing several cars ahead.

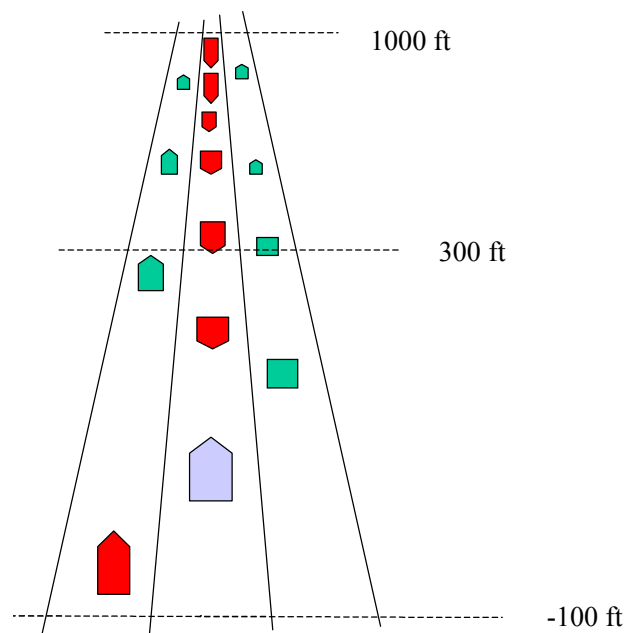


**Figure 10:** Notional Design of a Heads-Up Display for Driver Situation Awareness

### Roadblocks

An essential element of using RTK GPS is an accurate road database. Currently, in the US the databases are accurate to about 15 meters and do not contain altitude data. Japan and parts of Europe have databases that approach one meter accuracy. The development, monitoring, and updating of the required database will be a major undertaking [Wilson et al., 1998].

A current deterrent to using RTK GPS in production autos is the high cost of L1/L2 receivers. The cost is primarily because of the low production rate. If production rates were higher, the cost for an L1/L2 receiver should not be more than the cost of an L1 receiver. Since a GPS receiver primarily consists of signal processing hardware, most of the cost should continue to fall at a rate similar to

Moore's law for semiconductors (prices falling by 50% every 18 months). The of the receiver that is the exception is the radio frequency filters, which will remain analog for some time and keep the receivers from falling quite as rapidly as Moore's law [Ashjaee, 2001].

Currently, the demand for civilian GPS receivers is low, so production is on the order of tens of thousands per year for precision farming, surveying, and research. The market that could radically change this situation is the automotive market, which could potentially use tens of millions of these receivers per year if the cost is low enough. However, the automotive market cannot use these receivers until the cost is low. This conundrum hinders progress for both the GPS and automotive industries.

## ACKNOWLEDGMENTS

The author wishes to acknowledge Randy Galijan and Joe Strus in helping to gather and process the experimental data. They, along with Earl Blackwell, also contributed many helpful suggestions in designing the experiments and reviewing this paper.

## REFERENCES

- Ashjaee, J. [2001] GPS: The Challenge of a Single Chip. *GPS World* (May), pp. 24–27.
- De Jonge, P., and C. Tiberius [1996] The LAMBDA Method for Integer Ambiguity Estimation: Implementation Aspects. LGR-Series No. 12, Publications of the Delft Computing Centre.
- Hatch, R. [1990] Instantaneous Ambiguity Resolution. *Proceedings of the KIS Symposium, Banff, Canada.*
- Ibrahim, F., T. Pilutti, N. Al-Holou, and M. Paulik [1999] Accurate Gap Filling Using Properly Initialized INS during Periods of GPS Signal Blockage. *ION-GPS 1999*, pp. 1931–1940, Nashville, TN.
- Leick, A. [1995] *GPS Satellite Surveying*. 2<sup>nd</sup> edition, John Wiley & Sons, New York.
- Taniura, K., K. Fuse, and S. Takahashi [1998] Instantaneous Dual Frequency Ambiguity Resolution. *Institute of Navigation, ION-NTM-98*, pp. 781–790, Long Beach, CA.
- Sinko, J.W., R.C. Galijan, and T.M. Nguyen [1999] Centimeter-Level GPS for Highway Systems. 6<sup>th</sup> World Congress on Intelligent Transportation Systems, Toronto, Canada.
- Teunissen, P.J.G. [1994] A New Method for Fast Carrier Phase Ambiguity Estimation. *Proceedings IEEE Position, Location and Navigation Symposium PLANS 1994*, Las Vegas, NV, April 11–15, pp. 562–573.
- Venhovens, P., J. Bernasch, J. Lowenau, H. Rieker, and M. Schraut [1998] The Application of Advanced Vehicle Navigation in BMW Driver Assistance Systems. 99PC-240 (Society of Automotive Engineers, Inc.).

- Wilson, C., S. Rogers, and S. Weisenburger [1998] The Potential of Precision Maps in Intelligent Vehicles. *IEEE Intelligent Transportation Systems.*
- Yang, Y., J. Farrell, and H.S. Tan [2001] Carrier Phase Differential GPS-Aided INS Based Vehicle Control: Experimental Results. *ION NTM 2001*, Long Beach, CA, pp. 679–689.